

Prediction of aftershocks with Gaussian process regression

Kosuke Morikawa¹, Hiromichi Nagao^{2,3}, Shin-ichi Ito^{2,3}, Yoshikazu Terada^{1,4},
Shin'ichi Sakai^{2,5} and Naoshi Hirata^{2,6}.

¹ *Graduate School of Engineering Science, Osaka University, 1-3, Machikaneyama-cho, Toyonaka-shi, Osaka 560-8531, Japan.*

² *Earthquake Research Institute, The University of Tokyo, 1-1-1, Yayoi, Bunkyo-ku, Tokyo 113-0032, Japan.*

³ *Graduate School of Information Science and Technology, The University of Tokyo, 7-3-1, Hongo, Bunkyo-ku, Tokyo 113-8656, Japan.*

⁴ *Center for Advanced Intelligence Project, RIKEN, 1-4-1, Nihonbashi, Chuo-ku, Tokyo 103-0027, Japan.*

⁵ *Interfaculty Initiative in Information Studies Graduate School of Interdisciplinary Information Studies, The University of Tokyo, 7-3-1, Hongo, Bunkyo-ku, Tokyo 113-0033, Japan.*

⁶ *National Research Institute for Earth Science and Disaster Resilience, 3-1, Tennodai, Tsukuba-shi, Ibaraki 305-0006, Japan.*

SUMMARY

Uncovering the distribution of magnitudes and arrival times of aftershocks is a key to comprehend the characteristics of the sequence of earthquakes, which enables us to predict seismic activities and hazard assessments. However, identifying the number of aftershocks immediately after the main shock is practically difficult due to contaminations of arriving seismic waves. To overcome the difficulty, we construct a likelihood based on the detected data incorporating a detection function to which the Gaussian process regression (GPR) is applied. The GPR is capable of estimating not only the parameters of the distribution of aftershocks together with the detection function but also credible intervals for

both of the parameters and the detection function. A property that distributions of both the Gaussian process and aftershocks are exponential functions leads to an efficient Bayesian computational algorithm to estimate the hyperparameters. After the validations through numerical tests, the proposed method is retrospectively applied to the catalog data related to the 2004 Chuetsu earthquake towards early forecasting of the aftershocks. The result shows that the proposed method stably estimates the parameters of the distribution simultaneously their credible intervals even within three hours after the main shock.

Key words: Aftershock distribution; detection function; point process; Gaussian process regression.

1 INTRODUCTION

A massive earthquake triggers a number of aftershocks. The classical representative models to describe the temporal distribution of aftershocks were established as the Omori-Utsu (Omori 1894; Utsu 1961) and the Gutenberg-Richter (Gutenberg & Richter 1944) formulae, the latter of which also considered the information of magnitudes. Ogata (1988) proposed, having extended the Omori-Utsu formula, the Epidemic Type Aftershock Sequence (ETAS) model to describe more realistically that large aftershocks also excite subsequent aftershocks like the main shock. The distribution of aftershocks enables us to forecast seismic activities and hazard assessments (Resenberg & Jones 1989, 1994; Kagan & Jackson 2000). Until now, previous studies have proposed many statistical methods to estimate the parameters involved in the models (Aki 1965; Ogata 1983, 1988). A disadvantage of these parameter estimation methods is that they assume the existence of complete data without missing. However, detecting all aftershocks immediately after the main shock is unrealistic due to contaminations of a tremendous amount of seismic waves. Such incomplete data cause underestimations in the counting of aftershocks.

In statistics, situations in which only some detected data being available are known as biased sampling problems (Vardi 1982, 1985). In our case, the detection probability of aftershocks clearly depends on the magnitudes and elapsed times from the main shock. This type of biased sampling data is termed as missing not at random (MNAR), in which the detection probability depends on the values of undetected data. Introducing a detection function, which is a model of the detection probability, enables us to correct the bias (Qin 2017). Several studies have tackled this problem by introducing a parametric model on the detection function for aftershocks (Ringdal 1975; Ogata & Katsura 1993, 2006; Omi et al. 2013, 2014, 2015a,b). The detection function enables us to construct valid estimators

in MNAR. Three problems remain to be solved: (i) the resulting estimators are often unstable; (ii) misspecification of the detection function causes bias; (iii) estimation of the detection function is difficult even with a correct model. The problem (i) arises from the simultaneous estimation of the detection function and the distribution of aftershocks. The problem (ii) is obvious because the bias correction strongly depends on how close the defined detection function to the true one is. The problem (iii) is because some integration is required in the likelihood, which makes estimations difficult in the biased sampling problems. In this study, we propose a nonparametric Bayesian estimator to overcome these three problems. Appropriate prior information considering characteristics of seismic activities in a target area improves the problem (i). A modeling of the detection function based on the technique of Gaussian Process Regression (GPR), which enables us to estimate an arbitrary continuous function from a given dataset without assuming a specific functional form, solves the problems (i) and (ii) simultaneously. The GPR has been accepted widely in the recent machine learning researches due to its flexibility and wide coverage of function spaces (Rasmussen et al. 2006; de G. Matthews et al. 2018). As for computation of the model parameters, we propose an efficient Bayesian estimation algorithm utilizing the property that distributions of both the Gaussian process (GP) and aftershocks are exponential functions, which are compatible to compute solving the third problem (iii).

Another advantage in the GPR is that it is capable of evaluating uncertainties or credible intervals of the estimated parameters naturally, which has been hard in the previous works in spite that knowing the uncertainty is inevitable to decide statistical decision. In summary, the proposed method can solve the three problems mentioned above and has an additional property that can estimate the uncertainties of the parameters.

This paper is organized as follows. Section 2 introduces the GPR, and proposes a method to estimate parameters for distribution of aftershocks with a detection function through the GPR. Section 3 validates the proposed method through numerical tests. Section 4 demonstrates the effectiveness of the proposed method by applying to the catalog data of the 2004 Chuetsu earthquake. Section 5 concludes the present study including perspective future works.

2 METHODOLOGY

The present paper proposes to use a detection function based on the GPR to model temporal changes in the detection probability of aftershocks even immediately after a main shock. This section first gives a brief explanation of the GPR, and then introduces the proposed method, especially its theoretical properties and an efficient computational algorithm.

2.1 Gaussian process regression

Recent studies in the solid Earth science used the GPR to construct models from given data in the cases that the physical or chemical process that produced the data was unknown or too complicated. The GPR estimates a regression function simultaneously with its uncertainty through Bayesian non-parametric estimation. For example, Kuwatani et al. (2018) proposed to apply the GPR to interpolate the observed quantities of chemical compositions along with the radius of a rock. The estimated uncertainty often provides valuable information for observational or experimental design, such as a suggestion of times and/or places of the next new observations or measurements. The present study adopts the GPR to obtain a nonparametric regression function in the framework of Bayesian estimation.

We first briefly explain a GP, which the GPR bases. The fundamental statistics tells that, for a random variable, there exists a corresponding distribution that generates random “values”. The GP is an extension of this concept to a random function, i.e., there exists a corresponding distribution that generates random “functions”. The distribution of a GP is usually denoted as $\text{GP}(f_{\text{prior}}(\cdot), \mathcal{K}(\cdot, \cdot))$, where $f_{\text{prior}}(\cdot)$ is the mean function and $\mathcal{K}(\cdot, \cdot)$ is the variance function or “kernel”. The notation like $f(\cdot)$ is used in this paper to abbreviate arguments emphasizing that f is a function. A radial basis function is often chosen among various candidate functions for the variance function or kernel $\mathcal{K}(\cdot, \cdot)$:

$$\mathcal{K}(x_1, x_2) = \phi_1 \exp \left\{ -\frac{(x_1 - x_2)^2}{\phi_2^2} \right\} \quad (\phi_1, \phi_2 > 0), \quad (1)$$

where x_1 and x_2 are arbitrary real numbers. Another reason why this study adopts the radial basis function for the kernel is that it adequately covers an infinite-dimensional function space with only a few hyperparameters. See Rasmussen et al. (2006) for the detailed explanation of the GP including other kernel functions. Figure 1(a) illustrates three random “functions” generated from a $\text{GP}(f_{\text{prior}}(\cdot), \mathcal{K}(\cdot, \cdot))$ with $f_{\text{prior}}(x) = x^2$, $\phi_1 = 0.3$ and $\phi_2 = 0.3$. For any n points x_1, x_2, \dots, x_n , where n is an arbitrary positive integer, the GP is mathematically equivalent to $\mathbf{f} = (f(x_1), f(x_2), \dots, f(x_n))^{\top}$ computed from a sampled function $f(\cdot)$ that follows a multivariate normal distribution with mean $\mathbf{f}_{\text{prior}} = (f_{\text{prior}}(x_1), f_{\text{prior}}(x_2), \dots, f_{\text{prior}}(x_n))^{\top}$ and variance $\mathcal{K}_n = (\mathcal{K}(x_i, x_j))$. Here (a_{ij}) means a matrix having a_{ij} in its (i, j) -th element, and the superscript \top means transposition. Note that the variance of the value $f(x_i)$ at any point x_i is $\mathcal{K}(x_i, x_i) = \phi_1$, and triple of its standard error $3\sqrt{\phi_1}$ produces approximately 99.7% confidence interval for the GP shaded region in red in Figure 1(a). Figure 1(b) indicates that the values of the function $f_1(\cdot)$ (black line in Figure 1(a)) at arbitrary n points x_1, x_2, \dots, x_n follows a multivariate normal distribution $\mathcal{N}(\mathbf{f}_1, \mathcal{K}_n)$, where $\mathbf{f}_1 = (f_1(x_1), f_1(x_2), \dots, f_1(x_n))^{\top}$. Intuitively speaking, when the number of points n goes to infinity, a set of points forms the function $f_1(\cdot)$ that is a sample from the distribution of the GP. This

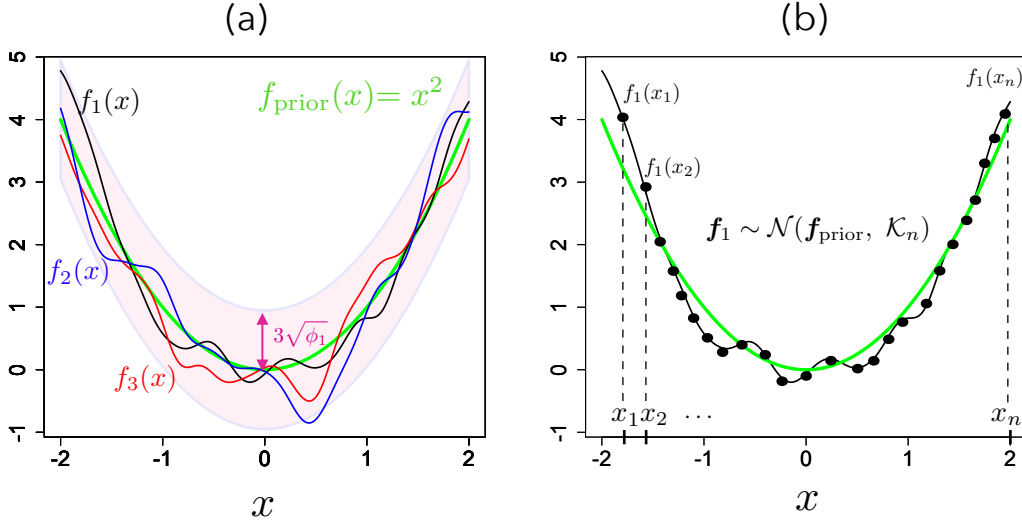


Figure 1. Example of GP: (a) three sampled functions generated from a GP with $f_{\text{prior}}(x) = x^2$ (green line), $\phi_1 = 0.3$, and $\phi_2 = 0.3$; (b) values of the function $f_1(\cdot)$ (black line in (a)) at arbitrary n points x_1, x_2, \dots, x_n . A set of these values forms a function sampled from the distribution of the GP when n goes to infinity.

consideration indicates that a GP is a stochastic process obtained by letting the dimension of a multivariate normal distribution go to infinity.

The GPR is a Bayesian estimation method for a target function by using a distribution of the GP as the prior information. Let $\mathbf{x} = (x_1, \dots, x_n)^\top$ and $\mathbf{y} = (y_1, \dots, y_n)^\top$ be sets of explanatory and response variables, respectively, and both are assumed to relate each other through an unknown regression function $f(\cdot)$, i.e., $y_i = f(x_i)$ ($i = 1, \dots, n$), where n denotes the number of time points. The GPR estimates the function $f(\cdot)$ from a given dataset assuming a kernel function mentioned above. We assume $\text{GP}(f_{\text{prior}}(\cdot), \mathcal{K}(\cdot, \cdot))$ as a prior distribution of the target function $f(\cdot)$. The mean function $f_{\text{prior}}(\cdot)$ is often assumed to be identically zero since the mean is adjustable by subtracting the sample mean of \mathbf{y} . Estimation of a function $f(\cdot)$ is equivalent to that of the value of $f(x^*)$ at any fixed point x^* , where the superscript “*” is used to discriminate the fixed point from the data points. A posterior distribution of $f^* = f(x^*)$ given a dataset $\mathcal{D} = \{x_1, \dots, x_n, y_1, \dots, y_n\}$ is called the predictive distribution. The Bayes’ theorem yields the predictive distribution as

$$p(f^* | x^*, \mathcal{D}) = \int p(f^* | x^*, \mathbf{f}, \mathcal{D}) p(\mathbf{f} | \mathcal{D}) d\mathbf{f}, \quad (2)$$

where $p(f^* | x^*, \mathbf{f}, \mathcal{D})$ is the conditional probability density function (PDF) of f^* with the given fixed point x^* , unobserved \mathbf{f} , and the dataset \mathcal{D} , and the PDF $p(\mathbf{f} | \mathcal{D})$ is the prior on \mathbf{f} given by a multivariate normal distribution $\mathcal{N}(\mathbf{f}, \mathcal{K}_n)$ as mentioned above. The predictive distribution becomes a normal distribution again. Therefore, the predictive distribution for a point x^* is a normal distribution

with mean $\mu_f(x^*)$ and variance $\sigma_f^2(x^*)$ computed as

$$\mu_f(x^*) = \boldsymbol{\kappa}_*^\top \mathcal{K}_n^{-1} \mathbf{y}, \quad \sigma_f^2(x^*) = \kappa_{**} - \boldsymbol{\kappa}_*^\top \mathcal{K}_n^{-1} \boldsymbol{\kappa}_*, \quad (3)$$

where $\mathcal{K}_n = (\mathcal{K}(x_i, x_j))$, $\boldsymbol{\kappa}_* = \{\mathcal{K}(x^*, x_1), \dots, \mathcal{K}(x^*, x_n)\}^\top$ and $\kappa_{**} = \mathcal{K}(x^*, x^*)$. The maximization of the marginal likelihood

$$\prod_{i=1}^n p(y_i | x_i; \phi) = \prod_{i=1}^n \int p(y_i | x_i, \mathbf{f}; \phi) p(\mathbf{f} | x_i; \phi) d\mathbf{f} \quad (4)$$

determines the hyperparameters $\phi = (\phi_1, \phi_2)$, where the integration in the right-hand side is explicitly computable since the integrand given as the product of normal distributions $p(y_i | x_i, \mathbf{f}; \phi)$ and $p(\mathbf{f} | x_i; \phi)$ is again a normal distribution. Figure 2 shows the predictive distributions estimated from six data points with changing hyperparameters ϕ_1 and ϕ_2 in the kernel (eq. 1). As mentioned above, the GPR successfully obtains not only the mean function but also its standard error i.e., credible interval. Figure 2 also indicates that ϕ_1 and ϕ_2 strongly associate with scale and shape of the regression function, respectively. A comparison between Figures 2(a) and 2(c), or 2(b) and 2(d) indicates that small/large ϕ_1 means a small large/credible interval. Another comparison between Figure 2(a) and 2(b), or 2(c) and 2(d) shows that small/large ϕ_2 means an oscillating/smoothed regression function. These results indicate the importance of deciding the hyperparameters.

2.2 Notation and models

According to the Omori-Utsu law, aftershock occurrence rate $n(t)$ at elapsed time t from the main shock follows a non-stationary Poisson process (Omori 1894; Utsu 1961):

$$n(t; \boldsymbol{\tau}) = \frac{K}{(t + c)^p}, \quad (5)$$

where $\boldsymbol{\tau}$ is a vector containing all the model parameters, i.e., $\boldsymbol{\tau} = (K, p, c)^\top$. The parameter K controls the level of seismic activity, i.e., large/small K reflects the large/small number of aftershocks. The parameter p is the slope of the occurrence rate in the logarithmic scale. The parameter c characterizes the length of capped time, which means the well-known phenomenon that the occurrence rate is below some level for a while immediately after the main shock (Utsu 1961; Ogata 1983). According to the Gutenberg-Richter law, the intensity rate of the magnitude M is described by an exponential function (Gutenberg & Richter 1944):

$$m(M; b) = A10^{-bM} \propto \exp(-\beta M), \quad (6)$$

where A and b (or $\beta = b \ln 10$) are constants. The parameter b is of the most interest since it reflects the intensity rate of magnitude in the statistical meaning. Combining eqs. (5) and (6), the joint occurrence

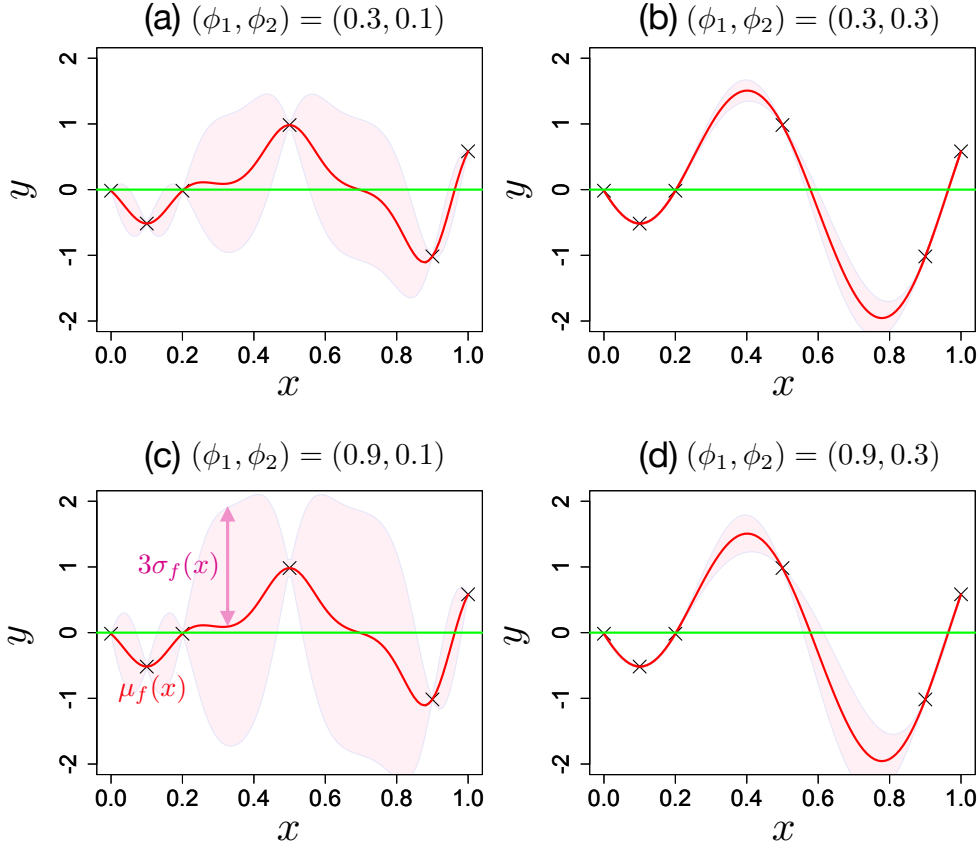


Figure 2. Gaussian process regression applied to six data points (“ \times ”) with different hyperparameters (ϕ_1, ϕ_2) . The green line is the mean function $f_{\text{prior}}(\cdot)$ of the prior distribution, which is assumed to be identically zero, the red curve is the estimated mean $\mu_f(\cdot)$ of the predictive distribution, and shaded region is the deviation $3\sigma_f(\cdot)$ from the mean of the predictive distribution.

rate of aftershocks as a function of elapsed time t and magnitude M is represented by the product of $n(t)$ and $m(M)$ as

$$\lambda(t, M; \boldsymbol{\tau}, \beta) = \frac{K'}{(t+c)^p} \beta e^{-\beta(M-M_0)}, \quad (7)$$

where $K' = \beta^{-1}KA \exp(-\beta M_0)$ and M_0 is the magnitude of the main shock used to adjust the scale of K' (Utsu 1970). Note that a unique decomposition into K and A is mathematically impossible, even if K' is obtained. Resenberg & Jones (1989, 1994) pointed out that an estimation of K' leads to forecast seismic activities, so that the unique decomposition problem does not matter in this context. Hereafter we use K instead of K' for notational simplicity.

An exact count of all aftershocks right after a main shock is too tough due to contaminations of arriving seismic waves, so that the occurrence rate of aftershocks is almost always underestimated. In order to correct the bias, the present study adopts the probit-type detection function as is used in Ringdal (1975), Ogata & Katsura (1993), Ogata & Katsura (2006), and Omi et al. (2013, 2014),

2015a,b):

$$\begin{aligned}\pi(t, M; \mu, s) &= P(\delta = 1 \mid t, M; \mu, s) \\ &= \int_{-\infty}^M \frac{1}{\sqrt{2\pi s^2}} \exp\left\{-\frac{(x - \mu(t))^2}{2s^2}\right\} dx,\end{aligned}\quad (8)$$

where δ is a detection indicator that takes 1/0 if the aftershock is detected/undetected, $\mu(t)$ is the magnitude that makes aftershock detectable with probability 50% at elapsed time t , and s is a scale parameter. Roughly speaking, the function $\mu(t)$ is decreasing with respect to the elapsed time t because only large aftershocks are detectable immediately after the main shock and even small aftershocks are detectable after enough time passes.

To distinguish the notations related to complete and detected data, let t_1 and M_1 be the elapsed time and magnitude of a detected aftershock, respectively. The subscript “1” indicates the detected data, i.e., $\delta = 1$. Note that t_1 and M_1 are always available though the complete data t and M are usually unavailable. Supposing that n aftershocks are detected, let the pair of elapsed time from the main shock and magnitude of i -th aftershock be (t_{1i}, M_{1i}) ($i = 1, \dots, n$). The thinning operation or the random deletion in point processes (Ogata & Katsura 1993) yields the likelihood function for the detected magnitudes

$$\begin{aligned}&\prod_{i=1}^n L(M_{1i} \mid t_{1i}; \beta, \mu, s^2) \\ &= \prod_{i=1}^n \frac{e^{-\beta M_{1i}} \pi(t_{1i}, M_{1i}; \mu, s^2)}{\int_{-\infty}^{\infty} e^{-\beta M} \pi(t_{1i}, M; \mu, s^2) dM} \\ &= \prod_{i=1}^n \beta \exp\left\{-\beta(M_{1i} - \mu(t_{1i})) - \frac{1}{2}\beta^2 s^2\right\} \pi(t_{1i}, M_{1i}; \mu, s^2),\end{aligned}\quad (9)$$

where the function $\mu(\cdot)$ is assumed to be known, although it is estimated later in practice. Using the estimated $\hat{\beta}$ and \hat{s} obtained by maximizing eq. (9), τ can be estimated by maximizing the log-likelihood function for detected elapsed times within any time interval $(0, T)$ (Ogata & Katsura 1993),

$$\sum_{0 < t_{1i} < T} \ln \nu(t_{1i}; \tau, \hat{\beta}, \hat{s}) - \int_0^T \nu(t; \tau, \hat{\beta}, \hat{s}) dt, \quad (10)$$

where $\nu(t)$ is an intensity function for detected data defined by

$$\begin{aligned}\nu(t; \tau, \beta, s) &= \int_{-\infty}^{\infty} \lambda(t, M; \tau, \beta) \pi(t, M; s) dM\end{aligned}\quad (11)$$

$$= \frac{K}{(t+c)^p} \exp\left\{-\beta(\mu(t) - M_0) + \frac{1}{2}\beta^2 s^2\right\}.\quad (12)$$

This paper proposes a more efficient estimation method for τ in Section 2.4, obtained from an investigation of the problem in the estimations of β and s as mentioned in Section 2.3.

However, a serious problem that $\mu(\cdot)$ is unknown remains. In frequentist ways, Ogata & Katsura (1993) applied a B-spline basis function to $\mu(\cdot)$, and Ogata & Katsura (2006) proposed a specific parametric model based on the 2003 Miyagi-Ken-Oki earthquake as

$$\mu(t) = a_0 + a_1 \exp \{-\alpha(3 + \ln t)^\gamma\}, \quad (13)$$

where a_0 , a_1 , α , and γ are parameters to be estimated. Recently, Omi et al. (2013) proposed a flexible nonparametric Bayesian estimation. They assumed a prior on $\mu(t_{1i})$ ($i = 1, \dots, n$), and computed the posterior mean. Their method does not require any specification of $\mu(\cdot)$ and it can naturally incorporate the prior information of β , which considerably makes estimates stable. The posterior distribution of β can be estimated in the same aftershock area that occurred before the main shock. However, their method never evaluates the credibility of $\mu(t_{1i})$ or β , which is inevitable to decide statistical decisions.

2.3 Estimation for β , s^2 , and $\pi(\cdot)$

Figure 3(a) shows a graphical model for complete data, which illustrates how the data, parameters, and hyperparameters relate to each other in accordance with the Omori-Utsu law, the Gutenberg-Richter law, and the detection function. Since the complete data are not available, we construct a likelihood based on the detected data M_1 given t_1 as shown in Figure 3(b). The distribution of M_1 given t_1 is already derived in eq. (9). Once the graphical model for the detected data was obtained, one would realize that relation among M_1 , μ , and t_1 is exactly the same as the regression: each input x , the regression $f(\cdot)$, and output y corresponds to t_1 , $\mu(\cdot)$, and M_1 , respectively. Based on this idea, we put a GP prior on $\mu(\cdot)$ and consider a nonparametric Bayesian estimation. However, unlike the GPR explained in Section 2.1, the distribution derived in eq. (9) is not a normal distribution, and the predictive distribution shall be more complicated.

In this study, we put a GP prior on the “function” $\mu(\cdot)$, not on the “points” $\mu(t_{1i})$ ($i = 1, \dots, n$). The GP prior leads to an explicit form of the marginal likelihood of hyperparameters and posterior distribution of $\mu(\cdot)$ as seen in the following discussion. The prior for $\mu(\cdot)$ can be denoted as $\mu \sim \text{GP}(\mu_{\text{prior}}(\cdot), \mathcal{K}(\cdot, \cdot))$, where \mathcal{K} is defined as

$$\mathcal{K}(x_1, x_2) = \phi_0 + \phi_1 \exp \left\{ -\frac{(x_1 - x_2)^2}{\phi_2} \right\} \quad (\phi_1, \phi_2 > 0). \quad (14)$$

The prior $\mu_{\text{prior}}(\cdot)$ should be a function except for identically zero in this case since adjusting the mean of the prior like in the GPR is impossible. Section 3 shows later that this simple prior works well through numerical experiments.

The first term ϕ_0 in eq. (14) is added to the usual kernel eq. (1) to make the matrix \mathcal{K}^{-1} always nonsingular. A subjectively small value, e.g., 10^{-7} , is set to ϕ_0 for a stable estimation of the other parameters. In summary, the parameters to be estimated are $\theta = (\beta, s^2, \phi_1, \phi_2)$.

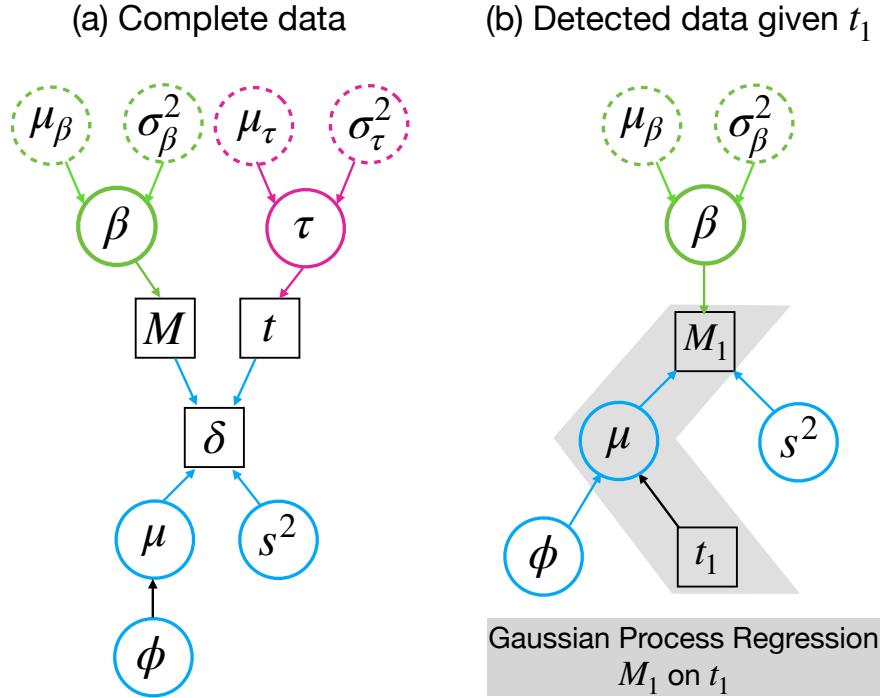


Figure 3. Graphical models on (a) complete data; (b): detected data given t_1 . Each square, circle, and dotted circle indicates data, parameters, and subjective hyperparameters, respectively. Each green, red, blue color indicates the relation by the Omori-Utsu law, the Gutenberg-Richter law, and the detection function, respectively.

Let $\theta_0 = (\mu_\beta, \sigma_\beta^2)$ be the hyperparameter of the subjective prior for β estimated in the same aftershock area that occurred before the main shock (Omi et al. 2013). The marginal likelihood of the hyperparameters and the predictive distribution of $\mu(\cdot)$ are computable as follows (see Appendix for the proofs).

- Marginal likelihood of $\theta = (\beta, s^2, \phi_1, \phi_2)$:

$$\begin{aligned}
 & p(\mathcal{D} \mid \theta) \\
 &= p(\theta; \theta_0) \int p(\mathbf{M}_1 \mid \mathbf{t}_1; \beta, \mu, s^2) p(\mu \mid \mathbf{t}_1; \phi_1, \phi_2) d\mu \\
 &= \beta^n \exp \left\{ -\beta \sum_{i=1}^n (\mathbf{M}_1 - \boldsymbol{\mu}_{\text{prior}})^\top \mathbf{1}_n - \frac{1}{2} \beta^2 \mathbf{1}_n^\top (s^2 \mathbf{I}_n - \mathcal{K}_n) \mathbf{1}_n \right\} \\
 &\quad \times p(\theta; \theta_0) \int_{\mathcal{M}} \mathcal{N}(\mathbf{x}; \tilde{\boldsymbol{\mu}}_n, \tilde{\mathcal{K}}_n) d\mathbf{x},
 \end{aligned} \tag{15}$$

where $\mathcal{M} = \otimes_{i=1}^n \{x_i \leq M_{1i}\}$ is the integration interval, $\otimes_{i=1}^n$ is the direct product of the n sets $\{x_i \leq M_{1i}\}$ ($i = 1, \dots, n$), $\tilde{\boldsymbol{\mu}}_n = \boldsymbol{\mu}_{\text{prior}} + \beta \mathcal{K}_n \mathbf{1}_n$, $\mathbf{1}_n$ is the n -dimensional vector that has one in its

all elements, $\tilde{\mathcal{K}}_n = \mathcal{K}_n + s^2 I_n$, I_n is the n -dimensional identity matrix, and $\mathcal{N}(\mathbf{x}; \boldsymbol{\mu}, \Sigma)$ is the PDF of the normal distribution with mean $\boldsymbol{\mu}$ and variance Σ .

- Predictive distribution of $\mu(\cdot)$:

$$\begin{aligned} & p(\mu^* | t_1^*, \mathcal{D}) \\ &= \int p(\mu^* | t_1^*, \boldsymbol{\mu}, \mathcal{D}) p(\boldsymbol{\mu} | \mathcal{D}) d\boldsymbol{\mu} \end{aligned} \quad (16)$$

$$= \mathbb{E}_{\text{trunc}} \left\{ \mathcal{N}(\mu^*; D^*(\mathbf{X}), (\tau^*)^2) \right\}, \quad (17)$$

where

$$D^*(\mathbf{x}) = (\mathbf{x} + s^2 \mathcal{K}_n^{-1} \tilde{\boldsymbol{\mu}}_n)^\top \left\{ (\tau^*)^2 \tilde{\mathcal{K}}_n^{-1} + \tilde{\mathcal{K}}_n^{-1} \boldsymbol{\kappa}_* \boldsymbol{\kappa}_*^\top \tilde{\mathcal{K}}_n^{-1} \right\} \frac{\boldsymbol{\kappa}_*}{\boldsymbol{\kappa}_{**}}, \quad (18)$$

$\boldsymbol{\kappa}_* = (\mathcal{K}(t_1^*, t_1), \dots, \mathcal{K}(t_1^*, t_n))^\top$, $\boldsymbol{\kappa}_{**} = \mathcal{K}(t_1^*, t_1^*)$, and $(\tau^*)^2 = \boldsymbol{\kappa}_{**} - \boldsymbol{\kappa}_*^\top \tilde{\mathcal{K}}_n^{-1} \boldsymbol{\kappa}_*$. The expectation $\mathbb{E}_{\text{trunc}}$ is on a variable $\mathbf{X} \sim \mathcal{TN}(\tilde{\boldsymbol{\mu}}_n, \tilde{\mathcal{K}}_n, \mathcal{M})$, where $\mathcal{TN}(\boldsymbol{\mu}, \Sigma, \mathcal{R})$ is the truncated multivariate normal distribution with mean $\tilde{\boldsymbol{\mu}}_n$, variance $\tilde{\mathcal{K}}_n$, bounded by the region \mathcal{R} . In particular, mean and variance of the predictive distribution are $D^*(\boldsymbol{\xi})$ and $(\tau^*)^2$, where

$$\boldsymbol{\xi} = \mathbb{E}_{\text{trunc}}(\mathbf{X}). \quad (19)$$

The symbol “*” explicitly represents that the variable depends on t_1^* .

- Predictive distribution of detection probability $\pi(\cdot)$:

$$\begin{aligned} & \pi^*(M_1^*, t_1^*) \\ &= \int P(\delta = 1 | M_1^*, \mu^*, \mathcal{D}) p(\mu^* | t_1^*, \mathcal{D}) d\mu^* \\ &= \mathbb{E}_{\text{trunc}} \left\{ \Psi \left(\frac{M_1^* - D^*(\mathbf{X})}{\sqrt{s^2 + (\tau^*)^2}} \right) \right\}, \end{aligned} \quad (20)$$

where $\Psi(\cdot)$ is the cumulative distribution function of the standard normal distribution, i.e., $\mathcal{N}(0, 1)$.

The integrations in eqs. (17), (19), and (20) are computable by the Monte Carlo method since they involve expectations on the known truncated multivariate normal distribution $\mathcal{TN}(\tilde{\boldsymbol{\mu}}_n, \tilde{\mathcal{K}}_n, \mathcal{M})$. However, computation of the integration in the marginal likelihood (eq. 15) is more difficult. We provide an efficient computational algorithm to obtain the posterior samples of the hyperparameter $\boldsymbol{\theta}$, instead of maximizing the marginal likelihood (eq. 15) directly.

2.4 Estimation for τ

Recall that the log-likelihood function for τ is given in eq. (10), but $\pi(\cdot)$ and $\mu(\cdot)$ are unknown in eq. (11) and eq. (12). Ogata & Katsura (1993) and Omi et al. (2013) replaced $\mu(\cdot)$ with the predictive distribution (eq. 16) based on eq. (12). The strong point in our procedure is that the detection function

in eq. (11) can be replaced with its predictive distribution already obtained in eq. (20). Our new approach using full information of the estimated detection function is expected to provide more efficient estimates, which is a significant advantage compared to the previous studies using only information of mean function $\mu(\cdot)$.

By replacing the detection function (eq. 11) with the predictive one (eq. 20), we have

$$\begin{aligned} & \nu^*(t; \tau, \beta, s) \\ &= \int_{-\infty}^{\infty} \lambda(t, M; \tau, \beta) \pi^*(t, M; s) dM \\ &= \frac{K}{(t+c)^p} \exp \left\{ \beta M_0 + \frac{1}{2} \beta^2 (s^2 + (\tau^*)^2) \right\} \mathbb{E}_{\text{trunc}} [\exp \{-\beta(D^*(\mathbf{X}))\}]. \end{aligned} \quad (21)$$

Computation of the expectation $\mathbb{E}_{\text{trunc}}$ by the distribution $\mathcal{TN}(\tilde{\boldsymbol{\mu}}_n, \tilde{\mathcal{K}}_n, \mathcal{M})$ is possible with the Monte Carlo method. As for the integration of the second term in eq. (10), we use a left Riemann sum discretizing t into 10^4 meshes having the same interval.

2.5 Computational algorithm

Both the predictive distribution and the marginal likelihood involve integration on multivariate normal distribution over an n -dimensional hyperrectangle \mathcal{M} . Since an explicit computation of the integral is hard even when the dimension is low (Genz & Bretz 2009), we divide the estimation into two steps: (i) estimation of hyperparameters $\boldsymbol{\theta}$; (ii) computation of mean and variance of the predictive distribution.

In the step (i), the data-augmentation method (Tanner & Wong 1987) is applied to obtain samples from the posterior distribution of $\boldsymbol{\theta}$. Regarding the variable \mathbf{x} in eq. (15) as a latent variable yields to another representation of the marginal likelihood as

$$p(\mathcal{D} | \boldsymbol{\theta}) = \int_{\mathcal{M}} p(\mathcal{D}, \mathbf{x} | \boldsymbol{\theta}) d\mathbf{x}, \quad (22)$$

where

$$\begin{aligned} & p(\mathcal{D}, \mathbf{x} | \boldsymbol{\theta}) \\ &= \beta^n \exp \left\{ -\beta(\mathbf{M}_1 - \boldsymbol{\mu}_{\text{prior}})^\top \mathbf{1}_n - \frac{1}{2} \beta^2 \mathbf{1}_n^\top (s^2 I_n - \mathcal{K}_n) \mathbf{1}_n \right\} \mathcal{N}(\mathbf{x}; \tilde{\boldsymbol{\mu}}_n, \tilde{\mathcal{K}}_n). \end{aligned} \quad (23)$$

In accordance with the Gibbs sampling, augmented data can be sampled via the following two steps:

- (i) Draw $\mathbf{x} \sim p(\mathbf{x} | \boldsymbol{\theta}, \mathcal{D}) = \mathcal{TN}(\mathbf{x}; \tilde{\boldsymbol{\mu}}_n, \tilde{\mathcal{K}}_n, \mathcal{M})$;
- (ii) Draw $\boldsymbol{\theta} \sim p(\boldsymbol{\theta} | \mathbf{x}, \mathcal{D}) \propto p(\mathcal{D}, \mathbf{x} | \boldsymbol{\theta}) p(\boldsymbol{\theta} | \boldsymbol{\theta}_0)$,

We apply the Gibbs sampling to obtain samples from the truncated normal distribution (Geweke 1991, 2005), and use the package `tmvtnorm` of R programming language (Wilhelm & Manjunath 2015) in the practical programming. As for sampling of $\boldsymbol{\theta}$, the classical random walk MCMC (Markov

Table 1. The true b and $\tau = (K, c, p)^\top$ in the numerical tests.

Case	b	$\ln(K)$	p	$\ln(c)$
1	0.9	8.700	1.100	-5.809
2	0.9	8.987	1.100	-5.809

Chain Monte Carlo) method (Metropolis et al. 1953) works with a normal distributions as the proposal distribution. By repeating the two steps alternately, obtained θ becomes samples from posterior of θ . Hyperparameters are estimated as the median of obtained samples. Once samples of \mathbf{x} are obtained, $\xi = \mathbb{E}_{\text{trunc}}(\mathbf{X})$ can be estimated by its sample mean. Mean of the predictive distribution of $\mu(\cdot)$ is computable with estimated ξ by $D^*(\xi)$ given in eq. (18), and variance is by $(\tau^*)^2$.

3 NUMERICAL EXPERIMENTS

We conduct numerical tests for the two cases of synthetic observation data to validate the performance of the proposed method. Table 1 summarizes the assumed true values for the parameters in the Omori-Utsu and the Gutenberg-Richter laws that are used to generate the two synthetic datasets. The magnitude of the main shock is assumed to be $M_0 = 6.0$.

The true detection functions modeled by eq. (8) in the two cases are

$$\begin{aligned} \text{Case 1. } \mu(t) &= \frac{1}{1 + 10t} + 1.3; \\ \text{Case 2. } \mu(t) &= 0.8 \frac{1 + \cos(5\pi t)}{1 + 4t} + 1, \end{aligned}$$

where the same scale parameter $s = 0.2$ is assumed for both cases. Figure 4(a) shows the true detection functions for both cases. Case 1 supposes an ordinary situation that the detectable magnitude of aftershocks monotonically decreases as the signal-to-noise ratio recovers with elapsed time from the main shock. Case 2 supposes a complicated situation that several large aftershocks excite many subsequent aftershocks again, and the detectable magnitude turns to increase for every large aftershock (Omi et al. 2013). We first estimate the predictive distribution of $\mu(\cdot)$ and β , and their credibility with data detected within 3, 6, 12, 24 hours. With the estimated $\hat{\mu}(\cdot)$, $\hat{\beta}$, and \hat{s} , τ is estimated by the method stated in Section 2.3. We assume $\mathcal{N}(1.0 \ln(10), 0.22)$ for the prior distribution of β , and no prior information for τ . Actually, the resulting estimates of τ would be stable without any prior distributions.

Figure 5 shows the estimated predictive distribution of $\hat{\mu}(\cdot)$. The mean of the predictive distribution is quite close to the true $\mu(\cdot)$ and inside a region within $3\hat{\sigma}(\cdot)$, where $\hat{\sigma}(\cdot)$ is the estimated standard error of $\hat{\mu}(\cdot)$. The resulting estimates with data (a) $t \leq 3$ are almost consistent with the case of (d) $t \leq 24$, which shows the robustness of our proposed method even with small datasets. It is

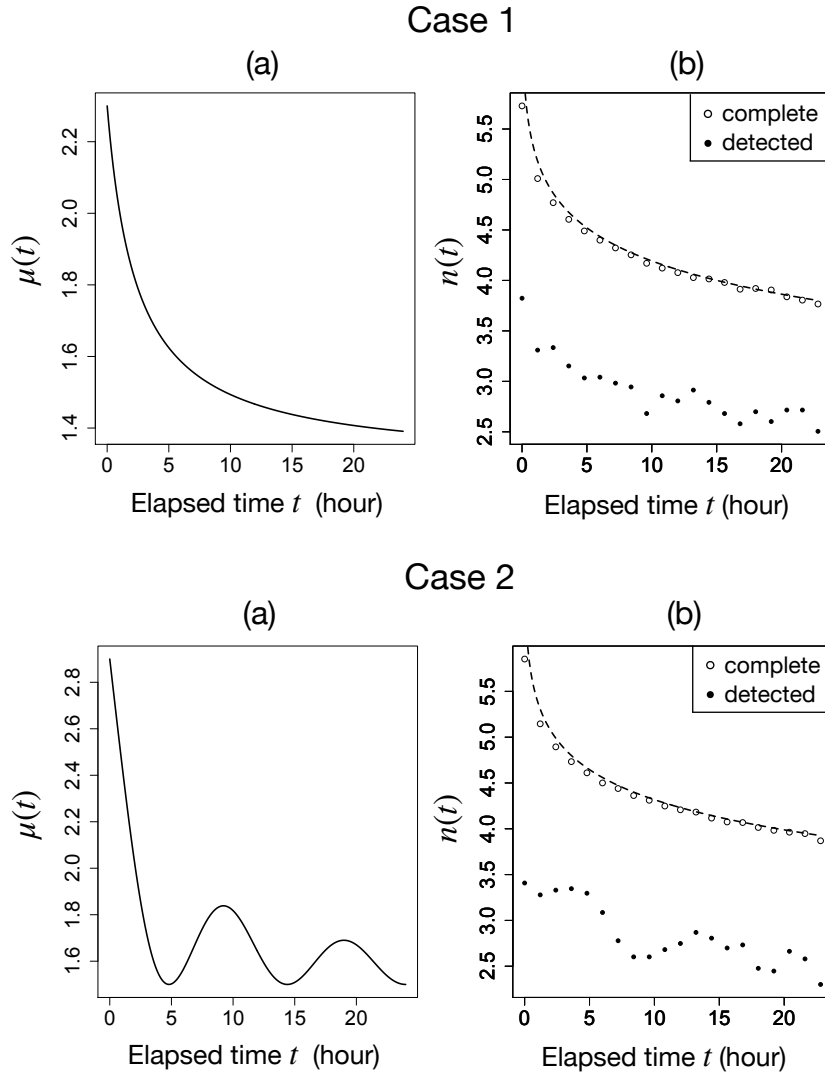


Figure 4. Synthetic data used in the numerical tests to validate the proposed method. (a) The mean $\mu(t)$ of the true predictive distribution. (b) The occurrence rate of aftershocks $n(t)$. The black solid and open circles indicate the complete and detected data, respectively, comparing to the true occurrence rate shown by the dashed line. See the text for the assumption for each of Cases 1 and 2.

worth noting that even if the mean of the prior distribution (green line) is not so similar to the true one (black dashed line), the predictive distribution reproduces the true $\mu(\cdot)$ considerably well. Table 2 summarizes the estimated \hat{b} and $\hat{\tau}$ comparing the proposed method (M1) with the method of Omi et al. (2014) (M2). The method M1 replaces the detection function $\pi(\cdot)$ with the predictive one in eq. (11), and the method M2 replaces $\mu(\cdot)$ with the estimated $\hat{\mu}(\cdot)$ in eq. (12). The estimates obtained by both methods are almost consistent. But in Case 2, M2 seems to fail to estimate p and/or c with data $t \leq 12$, while M1 gives stable estimates as expected in Section 2.3. As the elapsed time increases, the mean of posterior samples closes to the true value, and the length of the credible interval becomes shorter.

Table 2. Estimated posterior means and standard errors of b and $\tau = (K, c, p)^\top$ in Cases 1 and 2 with two methods. M1: proposed method (replacing the detection function with predictive one); M2: a method used in previous studies (replacing μ function with predictive one (eq. 12))

	Elapsed time	Case 1				Case 2			
		$t \leq 3$	$t \leq 6$	$t \leq 12$	$t \leq 24$	$t \leq 3$	$t \leq 6$	$t \leq 12$	$t \leq 24$
	# of data	483	668	875	1135	275	539	695	925
M1	b	0.846 (± 0.047)	0.860 (± 0.043)	0.889 (± 0.038)	0.901 (± 0.037)	0.846 (± 0.053)	0.850 (± 0.044)	0.851 (± 0.040)	0.859 (± 0.038)
	$\ln(K)$	-5.482 (± 0.304)	-4.902 (± 0.160)	-4.342 (± 0.094)	-3.703 (± 0.057)	-5.193 (± 0.317)	-4.320 (± 0.140)	-3.753 (± 0.104)	-3.083 (± 0.062)
	p	1.158 (± 0.111)	1.155 (± 0.068)	1.108 (± 0.045)	1.081 (± 0.031)	1.103 (± 0.119)	1.022 (± 0.062)	1.063 (± 0.053)	1.055 (± 0.037)
	$\ln(c)$	-5.616 (± 0.437)	-5.649 (± 0.342)	-5.844 (± 0.288)	-5.950 (± 0.262)	-5.838 (± 0.574)	-6.298 (± 0.462)	-6.052 (± 0.419)	-6.057 (± 0.350)
M2	$\ln(K)$	-5.476 (± 0.302)	-4.906 (± 0.160)	-4.513 (± 0.077)	-3.701 (± 0.057)	-5.192 (± 0.315)	-4.316 (± 0.142)	-3.648 (± 0.085)	-3.077 (± 0.058)
	p	1.156 (± 0.110)	1.157 (± 0.068)	1.061 (± 0.035)	1.081 (± 0.031)	1.102 (± 0.118)	1.022 (± 0.063)	0.885 (± 0.037)	1.052 (± 0.034)
	$\ln(c)$	-5.621 (± 0.437)	-5.644 (± 0.342)	-6.443 (± 0.310)	-5.949 (± 0.250)	-5.849 (± 0.583)	-6.303 (± 0.457)	-7.554 (± 0.492)	-6.072 (± 0.385)

Estimated 95% credible intervals, computed by estimated mean $\pm 1.96 \times$ estimated standard error, successfully include the true b -value ($b = 0.9$) even data with $t \leq 3$ in both cases. The reason why the estimated b -values in Case 2 are underestimated for all periods of available data is not due to the imperfectness of the proposed method but due to the sampling bias.

4 REAL DATA ANALYSIS

The proposed method is applied to the real catalog data related to the 2004 Chuetsu earthquake officially released from the Japan Meteorological Agency (JMA). The 2004 Chuetsu earthquake (magnitude $M_0 = 6.8$, epicenter $37^\circ 17' 30''$ N, $138^\circ 52' 00''$ E) occurred in Niigata prefecture, Japan at 17h56m on October 23, 2004 (JST). Figure 6 shows the spatial distribution of aftershocks that occurred within 24 hours from the main shock. The dataset is perfectly the same as used in Omi et al. (2015b), in which the aftershocks occurred in a rectangle area having the lengths four times the Utsu-

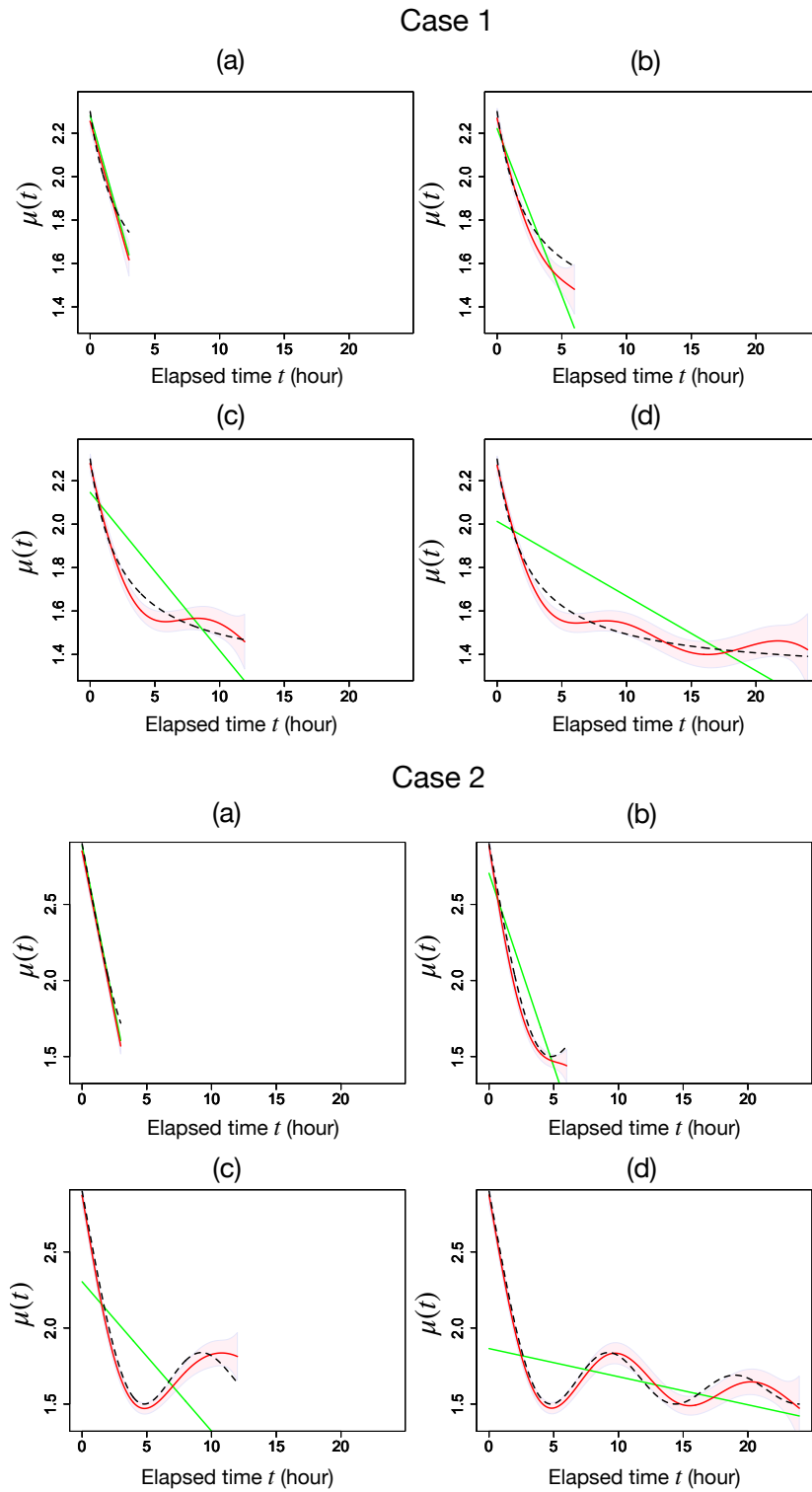


Figure 5. Results of numerical tests to validate the proposed method. The green line indicates the prior of the mean of the predictive distribution $\mu_{\text{prior}}(\cdot)$, and the red line indicates the estimated mean $\hat{\mu}(\cdot)$ with the estimation error $\hat{\mu}(\cdot) \pm 3\hat{\sigma}(\cdot)$ shown by the red shaded zone, comparing to the true mean $\mu(\cdot)$ shown by the dashed line, assuming that the data available for (a) 3 hours, (b) 6 hours, (c) 12 hours, and (d) 24 hours from the main shock.

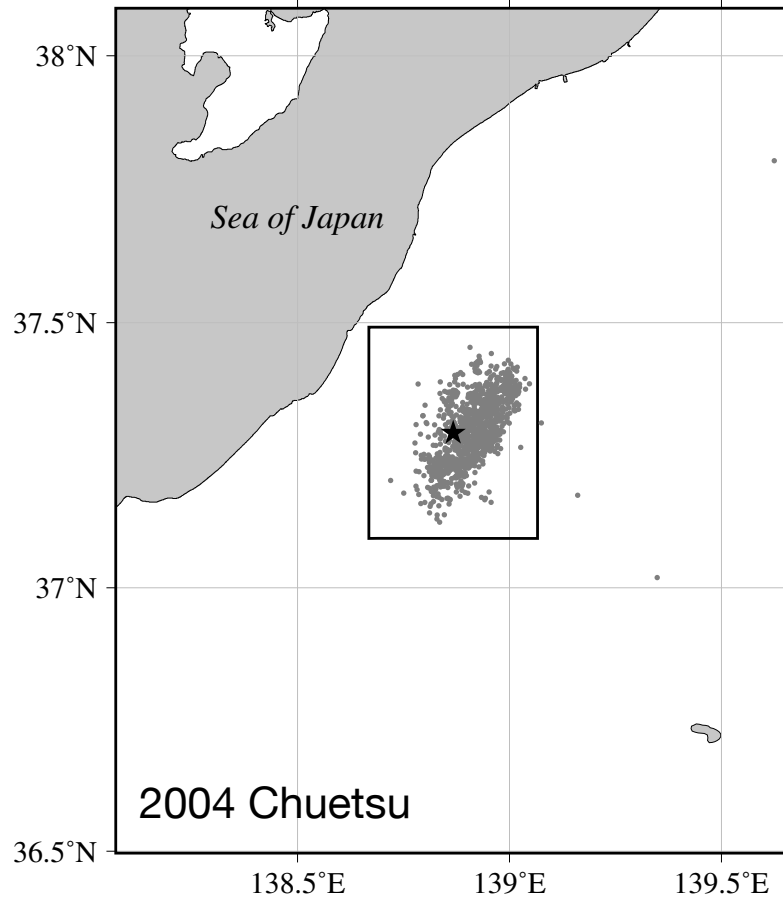


Figure 6. Spatial distribution of aftershocks (circle) within 24 hours from the main shock (star) of the 2004 Chuetsu earthquake officially released by JMA. The small rectangle is the Utsu-Seki aftershock zone, the center of which is the epicenter of the main shock, having the angle lengths of $2D(M_0)$ for both latitudinal and longitudinal directions, where $D(M_0)$ is the Utsu-Seki aftershock zone length.

Seki aftershock zone for latitudinal and longitudinal directions are selected. The Utsu-Seki aftershock zone is a rectangle region, in which the epicenter is located at the center, having the angle lengths of $2D(M_0)$ for both latitudinal and longitudinal directions, where $D(M_0)$ is the Utsu-Seki aftershock zone length defined using the magnitude of the main shock M_0 as $D(M_0) = 0.01 \times 10^{0.5M_0-1.8}$ (Utsu 1969). In the case of the 2004 Chuetsu earthquake, $D(M_0)$ is $23'53''$.

Figure 7 shows the results of applications to the real catalog data. Following the same procedure in the numerical tests in Section 3, the proposed method estimates the mean $\hat{\mu}(\cdot)$ of the predictive distribution with the standard error $\hat{\sigma}(\cdot)$ starting from the prior $\mu_{\text{prior}}(\cdot)$, assuming that the data available for 3, 6, 12, and 24 hours from the main shock. The magnitudes of aftershocks are ranging from 0.8 to 6.6 by the elapsed time of 24 hours.

The $\hat{\mu}(\cdot)$ is found not to simply decrease but turn to increase at $t = 12$ beyond the estimated

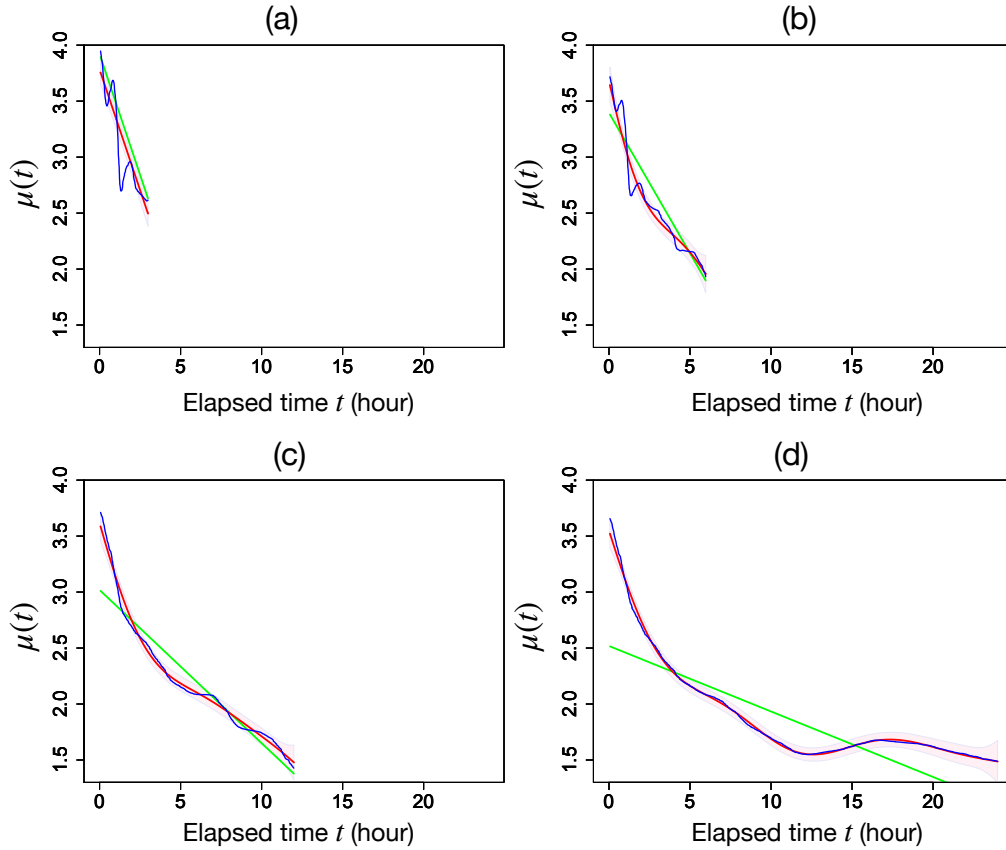


Figure 7. Results of application of our method to the 2004 Chuetsu earthquake. The green line indicates the prior of the mean of the predictive distribution $\mu_{\text{prior}}(\cdot)$, and the red line indicates the estimated mean $\hat{\mu}(\cdot)$ with the estimation error $\hat{\mu}(\cdot) \pm 3\hat{\sigma}(\cdot)$ shown by the red shaded zone, comparing to the mean $\mu(\cdot)$ estimated by Omi et al. (2014) shown by the blue line, assuming that the data available for (a) 3 hours, (b) 6 hours, (c) 12 hours, and (d) 24 hours from the main shock.

credible interval $\hat{\mu}(\cdot) \pm 3\hat{\sigma}(\cdot)$. One possible reason for this may be the fact that a large aftershock occurred at $t = 10.06$ with the magnitude of 4.8. The proposed method can extract such a hidden structure without missing, owing to a stable estimation of $\mu(\cdot)$.

The estimated $\mu(\cdot)$ by Omi et al. (2014) shown in Figure 7 for comparison seems to be unstable when available data are insufficient (Figures 7(a) and 7(b)), which is caused by some approximation methods for the marginal likelihood (supporting information of Omi et al. (2014)), although it is improved when the available data were extended to 24 hours. A similar phenomenon is also seen in Figure 3 in Omi et al. (2013). The proposed method always obtains a stable estimation even when the elapsed time is short (Figures 7(a) and 7(b)) owing to the exclusion of any approximations for the marginal likelihood (eq. 15). Figure 8(a) shows the estimated predictive detection function (eq. 20) in the case of the 2004 Chuetsu earthquake, and Figure 8(b) plots its cross-sections at the magnitudes $M = 0.8, 1.8, 2.3,$ and 2.8 . These magnitudes correspond to the minimum (0th percentile), 25th

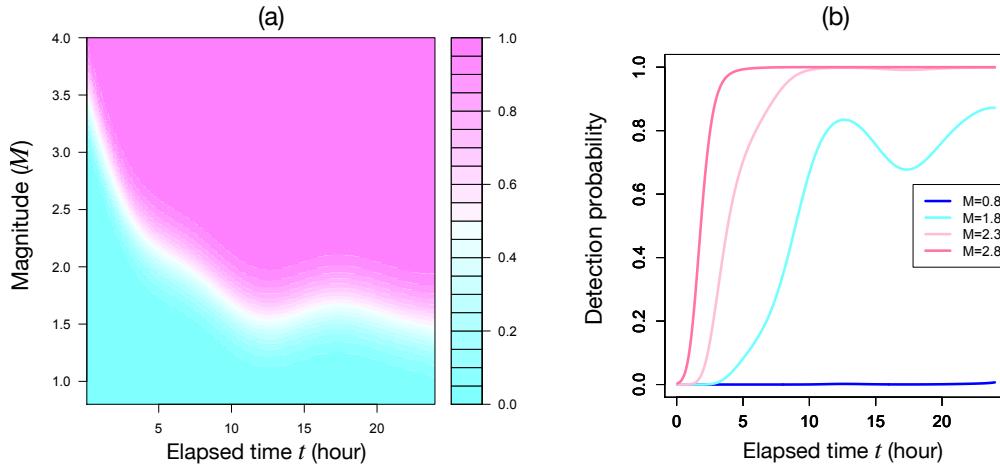


Figure 8. Estimated predictive distribution of detection function $\pi^*(M_1^*, t_1^*)$ with the application of the proposed method to the catalog data related to the 2004 Chuetsu earthquake: (a) predictive distribution of detection probability; (b) cross-sections of the predictive distribution of detection probability at the magnitudes $M = 0.8, 1.8, 2.3, 2.8$.

percentile, median (50th percentile), and 75th percentile in the catalog data, where q th-percentile is the magnitude below which $q\%$ of all the aftershocks are found. Figure 8(b) indicates that aftershocks with magnitudes larger than 2.3 are completely detected after $t \geq 10$, except $15 < t < 20$ when the detection probability is slightly less than 1 probably due to a large aftershock mentioned above.

Table 3 summarizes the mean and the standard error of the posterior distribution of b within elapsed time 3, 6, 12, and 24 hours. The estimates for the b -value are stable irrespective to the time available. On the other hand, the estimates of p and c with 24 hours are significantly small compared to the estimates with $t \leq 3, 6, 12$. This indicates that our method is successful in detecting the changes of seismic activity due to the large aftershock at $t = 10.06$.

5 CONCLUDING REMARKS

Immediate prediction of seismic activities after the main shock is important to assess hazards for subsequent aftershocks. Contaminations of arriving seismic waves right after the main shock interfere with counting the number of the aftershocks correctly, so that the number of detected aftershocks is underestimated. This underestimated count of the aftershocks causes distorted estimates for the distribution of the aftershocks or the seismic activities. In order to rapidly and stably estimate the temporal changes in the occurrence rate of aftershocks with limited data right after a main shock, we introduced a GPR-based detection function for the aftershocks to remove the effects of undetected aftershocks. Owing to the nonparametric and Bayesian properties in the GPR, the proposed detection function has

Table 3. Estimated posterior means and standard errors of b and $\boldsymbol{\tau} = (K, p, c)^\top$ in the case of the 2004 Chuetsu earthquake.

Elapsed time	$t \leq 3$	$t \leq 6$	$t \leq 12$	$t \leq 24$
# of data	192	355	655	1099
b	0.787 (± 0.066)	0.745 (± 0.051)	0.794 (± 0.045)	0.779 (± 0.035)
$\ln(K)$	-3.795 (± 0.438)	-3.129 (± 0.264)	-2.822 (± 0.117)	-1.658 (± 0.045)
p	1.529 (± 0.243)	1.484 (± 0.188)	1.537 (± 0.123)	1.270 (± 0.045)
$\ln(c)$	-3.573 (± 0.478)	-3.589 (± 0.492)	-3.509 (± 0.391)	-3.987 (± 0.362)

four advantages superior to the previous methods: (i) the resulting estimates are stable by virtue of adoption of prior information; (ii) specification of the detection function is not necessary; (iii) MCMC sampling is effective to compute the hyperparameters without computation of complicated integration; (iv) credible intervals can be obtained in a natural way.

The limitation of the proposed method is in the assumption on the joint intensity function (eq. 7). It is known that real catalog data should be described by more complicated intensity functions such as represented by the ETAS model (Ogata 1988). The proposed method can be extended straightforwardly to the ETAS model as done by Omi et al. (2014), which remains as a future work.

ACKNOWLEDGMENTS

This work was mainly supported by Tokyo Metropolitan Resilience Project of National Research Institute for Earth Science and Disaster Resilience (NIED), and partially supported by JST CREST Grant Numbers JPMJCR1763 and JPMJCR1761 of Japan Science and Technology Agency (JST). The key ideas in this study came through the activities of KAKENHI Grant-in-Aids for Early-Career Scientists No. 19K14592, 19K14671, 20K19756, Grant-in-Aids for Scientific Research (B) No. 17H01703, 17H01704, 18H03210, and Grant-in-Aid for Scientific Research (S) No. 19H05662. The travel expense needed to discuss among co-authors was partially supported by ERI JURP 2020-A-05. One of the figures was drawn by using the General Mapping Tools (GMT) developed by Wessel & Smith (1998).

REFERENCES

- Aki, K., 1965. Maximum likelihood estimate of b in the formula $\log N = a - bM$ and its confidence limits, *Bull. Earthq. Res. Inst. Univ. Tokyo*, **43**, 237–239.
- de G. Matthews, A. G., Rowland, M., Hron, J., Turner, R. E., & Ghahramani, Z., 2018. Gaussian process behaviour in wide deep neural networks, *arXiv preprint: 1804.11271*.
- Genz, A. & Bretz, F., 2009. *Computation of Multivariate Normal and t Probabilities. Lecture Notes in Statistics.*, Heidelberg: Springer.
- Geweke, J. F., 1991. Efficient simulation from the multivariate normal and student- t distributions subject to linear constraints and the evaluation of constraint probabilities, *Computer Science and Statistics. Proceedings of the 23rd Symposium on the Interface*. Seattle Washington, April 21-24, 1991, 571–578.
- Geweke, J. F., 2005. *Contemporary Bayesian Econometrics and Statistics*, Wiley & Sons.
- Gutenberg, B. & Richter, C. F., 1944. Frequency of earthquakes in California, *Bull. Seism. Soc. Am.*, **34**, 185–188.
- Kagan, Y. Y. & Jackson, D. D., 2000. Probabilistic forecasting of earthquakes, *Geophys. J. Int.*, **143**, 438–453.
- Kuwatani, T., Nagao, H., Ito, S., Okamoto, A., Yoshida, K., & Okudaira, T., 2018. Recovering the past history of natural recording media by Bayesian inversion, *Phys. Rev. E*, **98**, 043311.
- Metropolis, N., Rosenbluth, A. W., Rosenbluth, M. N., & Teller, E., 1953. Equations of state calculations by fast computing machine, *J. Chem. Phys.*, **21**, 1087–1091.
- Ogata, Y., 1983. Estimation of the parameters in the modified omori formula for aftershock frequencies by the maximum likelihood procedure, *J. Phys. Earth*, **31**, 115–124.
- Ogata, Y., 1988. Statistical models for earthquake occurrences and residual analysis for point processes, *J. Amer. Statist. Assoc.*, **83**, 29–39.
- Ogata, Y. & Katsura, K., 1993. Analysis of temporal and spatial heterogeneity of magnitude frequency distribution inferred from earthquake catalogs, *Geophys. J. Int.*, **113**, 727–738.
- Ogata, Y. & Katsura, K., 2006. Immediate and updated forecasting of aftershock hazard, *Geophys. Res. Lett.*, **33**, L10305.
- Omi, T., Ogata, Y., Hirata, Y., & Aihara, K., 2013. Forecasting large aftershocks within one day after the main shock, *Sci. Rep.*, **3**, 2218.
- Omi, T., Ogata, Y., Hirata, Y., & Aihara, K., 2014. Estimating the ETAS model from an early aftershock sequence, *Geophys. Res. Lett.*, **41**, 850–857.
- Omi, T., Ogata, Y., Hirata, Y., & Aihara, K., 2015a. Intermediate-term forecasting of aftershocks from an early aftershock sequence: Bayesian and ensemble forecasting approaches, *J. Geophys. Res.*, **120**, 2561–2578.
- Omi, T., Ogata, Y., Shiomi, K., Enescu, B., Sawazaki, K., & Aihara, K., 2015b. Automatic aftershock forecasting: A test using real-time seismicity data in Japan, *Bull. Seismol. Soc. Am.*, **106**, 2450–2458.
- Omori, F., 1894. On the aftershocks of earthquake, *J. Coll. Sci. Imp. Univ. Tokyo*, **7**, 111–200.
- Petersen, K. B. & Petersen, M. S., 2012. The matrix cookbook, Technical report, Technical University of Denmark, 2007. URL <http://www2.imm.dtu.dk/pubdb/p.php?3274>.

- Qin, J., 2017. *Biased Sampling, Over-identified Parameter Problems and Beyond*, Singapore: Springer.
- Rasmussen, C. E., Williams, C. K. I., & Christopher, K. I., 2006. *Gaussian Processes for Machine Learning*, The MIT Press.
- Resenberg, P. A. & Jones, L. M., 1989. Earthquake hazard after a mainshock in California, *Science*, **243**, 1173–1176.
- Resenberg, P. A. & Jones, L. M., 1994. Earthquake aftershocks: Update, *Science*, **265**, 1251–1252.
- Ringdal, F., 1975. On the estimation of seismic detection thresholds, *Bull. Seism. Soc. Am.*, **65**, 1631–1642.
- Tanner, M. A. & Wong, W. H., 1987. The calculation of posterior distributions by data augmentation, *J. Am. Stat. Assoc.*, **82**, 528–540.
- Utsu, T., 1961. A statistical study on the occurrence of aftershocks, *J. Coll. Sci. Imp. Univ. Tokyo*, **30**, 521–605.
- Utsu, T., 1969. Aftershocks and earthquake statistics (I) — Some parameters which characterize an aftershock sequence and their interrelations —, *J. Fac. Sci., Hokkaido Univ., Ser. VII (Geophysics)*, **3**, 129–195.
- Utsu, T., 1970. Aftershocks and earthquake statistics (II) — Further investigation of aftershocks and other earthquake sequences based on a new classification of earthquake sequences —, *J. Fac. Sci. Hokkaido Univ., Ser. VII (Geophysics)*, **3**, 197–266.
- Vardi, Y., 1982. Nonparametric estimation in presence of length bias, *Ann. Stat.*, **10**, 616–620.
- Vardi, Y., 1985. Empirical distributions in selection bias models, *Ann. Stat.*, **13**, 178–203.
- Wessel, P. & Smith, W. H. F., 1998. New, improved version of generic mapping tools released, *Trans. Am. Geophys. Un.*, **79**, 579.
- Wilhelm, S. & Manjunath, B. G., 2015. *tmvtnorm: Truncated Multivariate Normal and Student t Distribution*, R package version 1.4-10.

APPENDIX A: THEORETICAL RESULTS

Lemma 1. (Formula of sum of two squared forms (Petersen & Petersen 2012, section 8.1.7)).

For any vectors \mathbf{m}_1 and \mathbf{m}_2 , and nonsingular matrices Σ_1 and Σ_2 , it holds that

$$\begin{aligned}
 & -\frac{1}{2}(\mathbf{x} - \mathbf{m}_1)^\top \Sigma_1^{-1}(\mathbf{x} - \mathbf{m}_1) \\
 & -\frac{1}{2}(\mathbf{x} - \mathbf{m}_2)^\top \Sigma_2^{-1}(\mathbf{x} - \mathbf{m}_2) \\
 & = -\frac{1}{2}(\mathbf{x} - \mathbf{m}_c)^\top \Sigma_c^{-1}(\mathbf{x} - \mathbf{m}_c) + C,
 \end{aligned} \tag{A.1}$$

where

$$\Sigma_c^{-1} = \Sigma_1^{-1} + \Sigma_2^{-1} \tag{A.2}$$

$$\mathbf{m}_c = (\Sigma_1^{-1} + \Sigma_2^{-1})^{-1}(\Sigma_1^{-1}\mathbf{m}_1 + \Sigma_2^{-1}\mathbf{m}_2) \tag{A.3}$$

$$C = \frac{1}{2}\mathbf{m}_c^\top \Sigma_c^{-1}\mathbf{m}_c - \frac{1}{2}(\mathbf{m}_1^\top \Sigma_1^{-1}\mathbf{m}_1 + \mathbf{m}_2^\top \Sigma_2^{-1}\mathbf{m}_2). \tag{A.4}$$

Proof of Eq. (15). The definition of the marginal likelihood is

$$L(\boldsymbol{\theta}) = p(\beta) \int \prod_{i=1}^n p(M_{1i} | \mu_i; \beta, s^2) p(\boldsymbol{\mu} | \boldsymbol{\mu}_{\text{prior}}, \mathcal{K}_n) d\boldsymbol{\mu}, \quad (\text{A.5})$$

where $\boldsymbol{\theta} = (\beta, s^2, \phi_2^2)^\top$, $\boldsymbol{\mu}_{\text{prior}} = (\mu_{\text{prior}}(t_{11}), \dots, \mu_{\text{prior}}(t_{1n}))^\top$ is mean of the prior distribution, and $\mathcal{K}_n = (\mathcal{K}(t_{1i}, t_{1j}))$ is variance of the prior distribution which is an n by n matrix. Hereafter we ignore $p(\beta)$ because it does not have effect on integration. Recall that definition of the conditional distribution of M_1 given μ is given in eq. (9). It follows from

$$\begin{aligned} & \exp(\beta\mu_i) \Phi(M_{1i}; \mu_i, s^2) \\ &= \frac{\exp(\beta\mu_i)}{\sqrt{2\pi s^2}} \int_{-\infty}^{M_{1i}} \exp\left\{-\frac{(x - \mu_i)^2}{2s^2}\right\} dx \\ &= \frac{\exp(s^2\beta^2/2)}{\sqrt{2\pi s^2}} \int_{-\infty}^{M_{1i}} \exp\left[\beta x - \frac{\{\mu_i - (x + s^2\beta)\}^2}{2s^2}\right] dx \end{aligned} \quad (\text{A.6})$$

that the conditional distribution can be rewritten as

$$\begin{aligned} & \prod_{i=1}^n p(M_{1i} | \mu_i; \beta, s^2) \\ &= \beta^n \exp\left\{-\beta \sum_{i=1}^n M_{1i} - \frac{n}{2}\beta^2 s^2\right\} \prod_{i=1}^n \exp(\beta\mu_i) \Phi(M_{1i}; \mu_i, s^2) \\ &= \frac{\beta^n \exp(-\beta \sum_{i=1}^n M_{1i})}{\sqrt{(2\pi)^n |\Sigma|}} \int_{\mathbf{x} \in \mathcal{M}} \exp(\beta \mathbf{1}^\top \mathbf{x}) \\ & \quad \times \exp\left[-\frac{1}{2}\{\boldsymbol{\mu} - (\mathbf{x} + \beta\Sigma\mathbf{1})\}^\top \Sigma^{-1} \{\boldsymbol{\mu} - (\mathbf{x} + \beta\Sigma\mathbf{1})\}\right] d\mathbf{x}, \end{aligned}$$

where $\Sigma = s^2 I_n$, I_n is n by n identity matrix, and $\mathcal{M} = \otimes_{i=1}^n \{x_i \leq M_{1i}\}$. Letting $\mathbf{m}_1 = \mathbf{x} + \beta\Sigma\mathbf{1}$, $\mathbf{m}_2 = \boldsymbol{\mu}_{\text{prior}}$, $\Sigma_1 = \Sigma$, and $\Sigma_2 = \mathcal{K}_n$ with the formula (eq. A.1), leads to

$$\begin{aligned} & L(\boldsymbol{\theta}) \\ &= \frac{\beta^n \exp(-\beta \sum_{i=1}^n M_{1i})}{\sqrt{(2\pi)^n |\Sigma|} \sqrt{(2\pi)^n |\mathcal{K}_n|}} \int_{\mathcal{M}} \exp(\beta \mathbf{1}^\top \mathbf{x}) \\ & \quad \times \int \exp\left\{-\frac{1}{2}(\boldsymbol{\mu} - \mathbf{m}_1)^\top \Sigma_1^{-1} (\boldsymbol{\mu} - \mathbf{m}_1)\right\} \\ & \quad \times \int \exp\left\{-\frac{1}{2}(\boldsymbol{\mu} - \mathbf{m}_2)^\top \Sigma_2^{-1} (\boldsymbol{\mu} - \mathbf{m}_2)\right\} d\boldsymbol{\mu} d\mathbf{x} \\ &= \frac{\beta^n \exp(-\beta \sum_{i=1}^n M_{1i})}{(2\pi)^n \sqrt{|\Sigma| |\mathcal{K}_n|}} \\ & \quad \times \int_{\mathcal{M}} \exp(\beta \mathbf{1}^\top \mathbf{x}) \sqrt{(2\pi)^n |\Sigma_c|} \exp(C) d\mathbf{x} \end{aligned} \quad (\text{A.7})$$

Next, we compute m_c , Σ_c , and C in the formula. It follows from the standard argument in linear

algebra that

$$\Sigma_c = (\mathcal{K}_n^{-1} + \Sigma^{-1})^{-1} = \mathcal{K}_n \tilde{\mathcal{K}}_n^{-1} \Sigma, \quad (\text{A.8})$$

$$\mathbf{m}_c = \Sigma_c \{ \Sigma^{-1}(\mathbf{x} + \beta \Sigma \mathbf{1}) + \mathcal{K}_n^{-1} \boldsymbol{\mu}_{\text{prior}} \}, \quad (\text{A.9})$$

$$\begin{aligned} C &= -\frac{1}{2} \boldsymbol{\mu}_{\text{prior}}^\top \tilde{\mathcal{K}}_n^{-1} \boldsymbol{\mu}_{\text{prior}} - \frac{1}{2} (\mathbf{x} + \beta \Sigma \mathbf{1})^\top \tilde{\mathcal{K}}_n^{-1} (\mathbf{x} + \beta \Sigma \mathbf{1}) \\ &\quad + \boldsymbol{\mu}_{\text{prior}}^\top (\mathcal{K}_n + \Sigma)^{-1} (\mathbf{x} + \beta \Sigma \mathbf{1}), \end{aligned} \quad (\text{A.10})$$

where $\tilde{\mathcal{K}}_n = \mathcal{K}_n + \Sigma$. Rearranging the integrand so that it becomes a quadratic form of \mathbf{x} , we have

$$\begin{aligned} L(\boldsymbol{\theta}) &= \frac{\beta^n}{\sqrt{(2\pi)^n |\tilde{\mathcal{K}}|}} \exp \left\{ -\beta \sum_{i=1}^n (M_{1i} - \mu_{\text{prior},i}) - \frac{\beta^2}{2} \mathbf{1}^\top (\Sigma - \mathcal{K}_n) \mathbf{1} \right\} \\ &\quad \times \int_{\mathcal{M}} \exp \left\{ -\frac{1}{2} (\mathbf{x} - \tilde{\boldsymbol{\mu}})^\top \tilde{\mathcal{K}}_n^{-1} (\mathbf{x} - \tilde{\boldsymbol{\mu}}) \right\} d\mathbf{x}, \end{aligned} \quad (\text{A.11})$$

where $\tilde{\boldsymbol{\mu}} = \boldsymbol{\mu}_{\text{prior}} + \beta \mathcal{K}_n \mathbf{1}$. This is the desired conclusion.

Proof of Eq. (17). Let t_1^* be any data point may not be in the dataset. What we need to compute is

$$\begin{aligned} &p(\mu^* | t_1^*, \mathcal{D}) \\ &= \int p(\mu^* | t_1^*, \boldsymbol{\mu}, \mathbf{t}_1) p(\boldsymbol{\mu} | \mathbf{t}_1, \mathbf{M}_1) d\boldsymbol{\mu} \\ &= \frac{\int p(\mu^* | t_1^*, \boldsymbol{\mu}, \mathbf{t}_1) p(\mathbf{M}_1 | \boldsymbol{\mu}) p(\boldsymbol{\mu} | \mathbf{t}_1) d\boldsymbol{\mu}}{\int p(\mathbf{M}_1 | \boldsymbol{\mu}) p(\boldsymbol{\mu} | \mathbf{t}_1) d\boldsymbol{\mu}}. \end{aligned} \quad (\text{A.12})$$

Here, denominator of the predictive distribution is exactly the same as the marginal likelihood which is already computed. Hence it remains to show the numerator becomes

$$\begin{aligned} &\beta^n \exp \left\{ -\beta \sum_{i=1}^n (M_{1i} - \mu_{\text{prior},i}) - \frac{1}{2} \beta^2 \left(ns^2 - \sum_{i,j} \mathcal{K}_{i,j} \right) \right\} \\ &\quad \times \int_{\mathcal{M}} \mathcal{N}(\mu^*; D(\mathbf{x}), \tau^2) \mathcal{N}(\mathbf{x}; \tilde{\boldsymbol{\mu}}_n, \tilde{\mathcal{K}}_n) d\mathbf{x}. \end{aligned} \quad (\text{A.13})$$

It is computed by using the formula (eq. A.1) with respect to $\boldsymbol{\mu}$ with some tedious calculus.

Proof of Eq. (20). It follows from the result of eq. (17) that

$$\begin{aligned}
 & P(\delta = 1 \mid M_1^*, t_1^*, \mathcal{D}) \\
 &= \int P(\delta = 1 \mid M_1^*, \mu^*, \mathcal{D}) p(\mu^* \mid t_1^*, \mathcal{D}) d\mu^* \\
 &= \int_{-\infty}^{\infty} \int_{-\infty}^M \mathcal{N}(z; \mu^*, s^2) \\
 &\quad \times \frac{\int_{\mathcal{M}} \mathcal{N}(\mu^*; D^*(\mathbf{x}), (\tau^*)^2) \mathcal{N}(\mathbf{x}; \tilde{\boldsymbol{\mu}}_n, \tilde{K}_n) d\mathbf{x}}{\int_{\mathcal{M}} \mathcal{N}(\mathbf{x}; \tilde{\boldsymbol{\mu}}_n, \tilde{K}_n) d\mathbf{x}} d\mu^* \\
 &= \int_{-\infty}^M \frac{\int_{\mathcal{M}} \mathcal{N}(z; D^*(\mathbf{x}), s^2 + (\tau^*)^2) \mathcal{N}(\mathbf{x}; \tilde{\boldsymbol{\mu}}_n, \tilde{K}_n) d\mathbf{x}}{\int_{\mathcal{M}} \mathcal{N}(\mathbf{x}; \tilde{\boldsymbol{\mu}}_n, \tilde{K}_n) d\mathbf{x}} dz \\
 &= \mathbb{E}_{\text{trunc}} \left\{ \Psi \left(\frac{M_1^* - D^*(\mathbf{X})}{\sqrt{s^2 + (\tau^*)^2}} \right) \right\}. \tag{A.14}
 \end{aligned}$$

Proof of Eq. (21). By using the Fubini's theorem, we have

$$\begin{aligned}
 & \nu^*(t; \tau, \beta, s) \\
 &= \int_{-\infty}^{\infty} \lambda(t, M; \tau, \beta) \mathbb{E}_{\text{trunc}} \left\{ \Psi \left(\frac{M - D^*(\mathbf{X})}{\sqrt{s^2 + (\tau^*)^2}} \right) \right\} dM \\
 &= \frac{K}{(t+c)^p} \int_{-\infty}^{\infty} \beta e^{-\beta(M-M_0)} \\
 &\quad \times \frac{\int_{-\infty}^M \mathcal{N}(z; D^*(\mathbf{x}), s^2 + (\tau^*)^2) dz \int_{\mathcal{M}} \mathcal{N}(\mathbf{x}; \tilde{\boldsymbol{\mu}}_n, \tilde{K}_n) d\mathbf{x}}{\int_{\mathcal{M}} \mathcal{N}(\mathbf{x}; \tilde{\boldsymbol{\mu}}_n, \tilde{K}_n) d\mathbf{x}} dM \\
 &= \frac{K}{(t+c)^p} \int_{-\infty}^{\infty} \int_z^{\infty} \beta e^{-\beta(M-M_0)} dM \\
 &\quad \times \frac{\mathcal{N}(z; D^*(\mathbf{x}), s^2 + (\tau^*)^2) \int_{\mathcal{M}} \mathcal{N}(\mathbf{x}; \tilde{\boldsymbol{\mu}}_n, \tilde{K}_n) d\mathbf{x}}{\int_{\mathcal{M}} \mathcal{N}(\mathbf{x}; \tilde{\boldsymbol{\mu}}_n, \tilde{K}_n) d\mathbf{x}} dz \\
 &= \frac{K}{(t+c)^p} \mathbb{E}_{\text{trunc}} \left[\exp \left\{ -\beta(D^*(\mathbf{x}) - M_0) + \frac{1}{2} \beta^2 (s^2 + (\tau^*)^2) \right\} \right], \tag{A.15}
 \end{aligned}$$

as desired.

This paper has been produced using the Blackwell Scientific Publications GJI L^AT_EX2e class file.